Effect of variation in microstructure on high temperature creep of Fe-Ni-Cr superalloy

Esah Hamzah[1], Maureen Mudang[2], Muhammad Adil Khattak[3]

[1), 2), 3)] *Faculty of Mechanical Engineering, Universiti Teknologi Malaysia,*
81310, UTM Skudai, Johor
[1)] *esah@fkm.utm.my (corresponding author);*
[2)] *maureentingsl@hotmail.com;* [3)] *adil@fkm.utm.my*

ABSTRACT

Fe-Ni-Cr or known as Incoloy 800H is a solid solution strengthened iron-nickel based superalloy which is extensively used in high temperature environment. Based on its advantages such as high strength and corrosion resistant at high temperatures, this alloy was selected as one of the potential candidate alloy for Generation IV supercritical water-cooled nuclear plant design and for nuclear reactor systems. The effect of grain size in creep strength and creep rate comes through the grain boundary sliding mechanism. This paper describes the effect of microstructural variation of Fe-Ni-Cr on the high temperature creep properties. The material was heat treated at temperature 1050°C and 1200°C followed by water quenching process. The grain size of the samples is 95.47μm for as-received, 122.81μm for solution treated at 1050°C and 380.95μm for solution treated at 1200°C. The creep damage investigation was carried out in the three different grain sizes of Fe-Ni-Cr superalloy at 900°C with stress at 90MPa and 100MPa. Rectangular section forms of specimens are used in the research. In all the tests conducted, the creep curves show primary, secondary and tertiary stages. The creep fracture mode was characterised by using optical and scanning electron microscope. It was found that larger grain size results in higher creep rate.

1. INTRODUCTION

Nickel-based superalloys with an exceptional combination of high temperature strength, toughness, and resistance to degradation in corrosive or oxidizing environments. These materials are widely used in aircraft, power-generation turbines, rocket engines, and other challenging environment, including nuclear power and chemical processing plants, such as turbine discs, for high pressure stages (Chateau 2010, Tresa 2006). Due to the significant importance of materials used in high-temperature services, Fe-Ni-Cr alloys are widely used to replace stainless steel by modifying and adding some other elements making it a heat-resistant alloys (Hui 2000). Incoloy 800 is a solid solution strengthened iron-nickel base superalloy which is extensively used in high temperature environment (Dehmolaei 2009). Incoloy 800 was

the first of these alloys and it was slightly modified to become Incoloy 800H. This modification was to control carbon (0.05-0.10w%) and grain size to optimize stress rupture properties. Austenitic alloy 800H has the same basic composition as Incoloy alloy 800 (Fe–20Cr–32Ni) but with significantly higher creep-rupture strength due to the grain size. The microstructure will show fully austenitic matrix containing several types of precipitates which are found in the austenitic matrix and grain boundaries (Dehmolaei 2009). Based on its advantages such as high strength and corrosion resistant at high temperatures, alloy 800H was selected as one of the potential candidate alloys for Generation IV supercritical water-cooled nuclear plant designs and also being considered for nuclear reactor systems (Gan 2006, Tan 2006) Reactor materials will be exposed to very high temperatures, intense neutron radiation, and corrosive environments and in many cases, all three at once. Thus, it is important to fully understand the creep damage behavior for the design and safety evaluation process of high temperature structural material. For this purpose, the effect of grain size on creep properties is important for the evaluation of the characteristics of this material.

Creep failure is a major safety concern for materials working under high temperature. Creep usually happens at temperature roughly higher than 0.4Tm, where Tm is the absolute melting temperature of the alloy (Abe 2008, John 2012). At temperature above 0.4Tm, the dislocation are thereby no longer constrain to move only in their slip planes, process of climb is the principle of this free dislocation movement (Bernasconi 1979). The most widely reported creep damage mechanisms that occur in the bulk of specimens or components are cavities growth at grain boundaries interactions (Chateau 2010). Several research have been conducted on the effect of grain size and most of them focused on the steady state creep rates with the change in materials grain size. Numerous of reports prove that by increasing the grain size, the creep rate will decrease or increase base on the experiment conditions, materials properties and role of the grain boundaries reacted. For stainless steel , Lee prove that as the grain size increase, the steady state creep rate decrease to a minimum value then increase from the intermediate grain size. This is because grain boundaries react as both dislocation barrier and dislocation source (Lee 2001).

Therefore, in this paper, the effect of variation in microstructure in term of grain size at high temperature creep properties of Incoloy 800H was investigated by considering the role of the grain boundary on the steady state creep rate.

2. MATERIAL AND METHODS

The as-received material known as Incoloy 800H in form of plate shape with chemical composition (wt. %) shown in Table 1 was used in this work. The specimens were cut by using EDM wire cut into rectangular form then followed by heat treatment process. The dimension of the specimens is referred to the ASTM E8. Table 2 shows the solution treatment conditions and grain sizes number. The specimens were subjected to various solution treatments temperature to produce different range of grain size which is determined by using the linear intercept method. Test machine MAYES TC 20 will be used for the creep test. The load on the specimen was applied as axially

as possible to ensure that the load is transferred to the specimen axially with minimum bending stresses arise. Constant load creep tests were carried out at 900°C in air using stress of 90MPa and 100MPa. Temperature controlled to ±3°C during creep tests. A linear variable differential transformer (LVDT) was used for measuring the strain elongation. The strain elongation versus time result is then used to plot the "S" creep curve. The slope of secondary stage in creep curves was taken as steady state creep rate. Scanning electron microscope was used to examine the fracture surface. In order to perform metallographic examination, the specimens were mechanically grinded, polished and etched in etching reagent followed the ratio, Glycerol (2): Hydrochloric Acid (3): Nitric Acid (1). Optical microscope was used to examine the cross section of the fracture specimens to observe the different grain shape at the fracture area and area away from the fracture zone.

Table 1: Composition of the material

Element	Fe	Ni	Cr	C	Si	Mn	Ti	Cu	S	Al	Al + Ti
Wt%	46.6	30.3	20.6	0.08	0.3	0.6	0.49	0.06	0.002	0.49	0.98

Table 2: Heat treatment and average grain sizes

Heat Treatment	Grain size (µm)
As-Received	95.47
1050°C/ 3hours + Water quench	122.81
1200°C/ 3hours + Water quench	380.95

3. RESULTS AND DISCUSSION

3.1 Effect of different solution treatment on microstructures

Figure 3.1 shows the microstructure and grain size for as-received material, specimens underwent solution treated at 1050°C and solution treated at 1200°C. The average of grain size of as-received specimen was 95.47µm, follow by 122.81µm for solution treated at 1050°C and 380.95µm for specimen underwent solution treatment at 1200°C. Increasing the solution treatment temperature will increase the average grain size. The microstructure shows austenitic matrix (Fe-Ni-Cr) with some precipitates i.e. Titanium Nitride (TiN) and Titanium Carbide (TiC) which is shown in Figure 3.2. It was found that the cubic shape of precipitates are rich in titanium and nitrogen and been identified as nitride or carbonitride of titanium which formed during the casting process. The irregular shape of precipitates are rich in titanium and carbon, and been identified as titanium carbide (TiC) (Dehmolaei 2009).
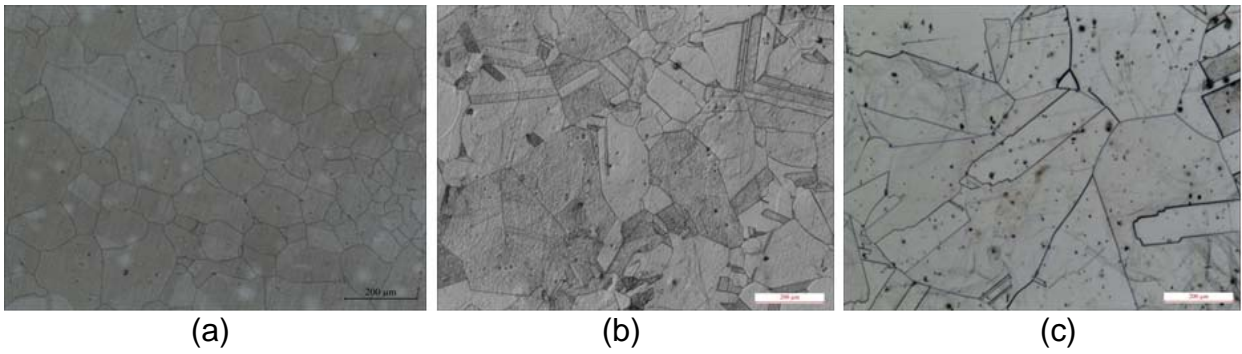
Figure 3.1. Microstructures of the specimens (50X). (a) As-received (b) Solution treated at 1050°C and (c) Solution treated at 1200°C.
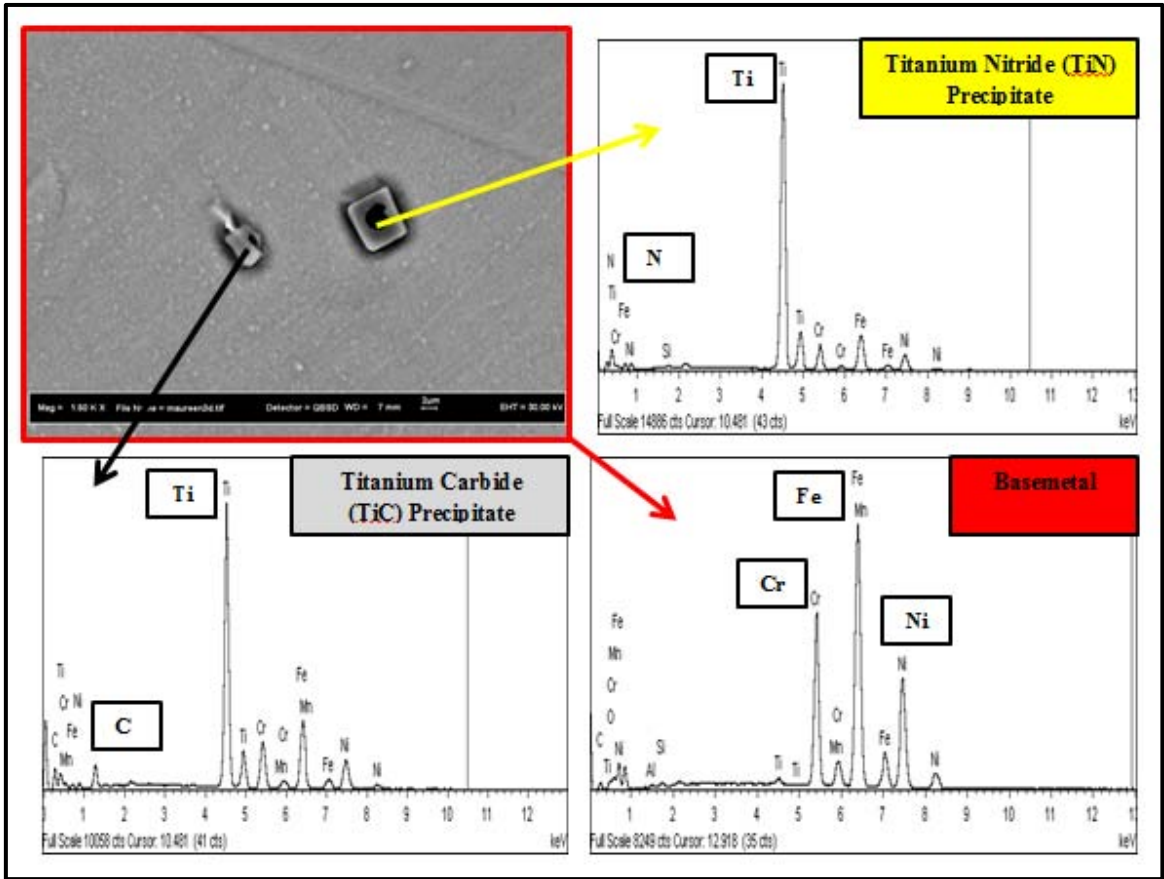

Figure 3.2. Energy-dispersive X-ray analysis of Fe-Ni-Cr alloy.

3.2 High Temperature Creep Test

The time for each specimen to rupture was first predicted by referring to Larson-Miller parameter curve (Voicu 2009). Constant stress test shows a typical pattern of

three stages creep strain behavior including primary stage, secondary stage, and tertiary stage. In the initial stage, or primary creep, the strain rate is relatively high, but slows down with increasing time. This is due to work hardening. The strain rate eventually reaches a minimum and becomes near constant. This is due to the balance between work hardening and annealing (thermal softening). This stage is known as secondary or steady state creep. In tertiary creep, the strain rate exponentially increases with stress because of necking phenomena. The time and elongation data were analyzed and expressed in terms of creep strain and time in a graph.

Figure 3.3 to 3.4 show that the creep pattern follows typical creep behavior where primary stage, secondary stage, and tertiary stage creep can be observed. This linear stage is called steady state creep or secondary creep. Eventually, this secondary creep reached a stage where creep rate accelerated rapidly. This region formed is called tertiary stage creep. As we can see from both of the graphs, the steady state creep rate and instantaneous strain both increase proportionally with the grain size.

Figure 3.3 shows three typical creep curve of Incoloy alloy 800H at 900°C, 90MPa. The steady state creep rate of as-received sample, specimen underwent solution treated at 1050°C and solution treated at 1200°C were 0.000310 %strain/s, 0.003568 %strain/s and 0.011936 %strain/s respectively. The instantaneous strain of as-received material, samples underwent solution treated at 1050°C and solution treated at 1200°C were 0.02 %strain, 0.06 %strain and 0.085 %strain. As we can see that, the creep rate and instantaneous strain increase with increased grain size.
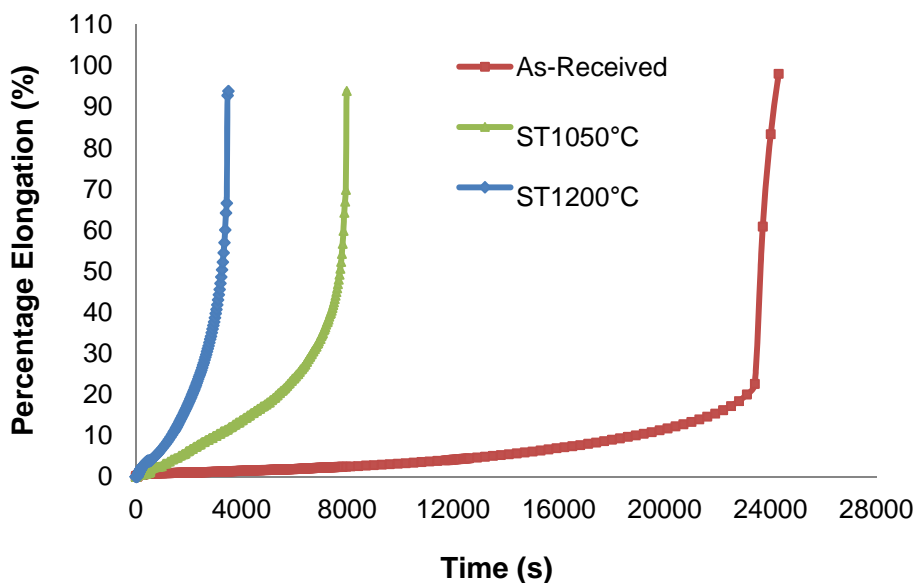

Figure 3.3. The creep curve of alloy 800H at 900°C and 90MPa stress.

Figure 3.4 shows three typical creep curve of Incoloy alloy 800H at 900°C, 100MPa. The steady state creep rate of as-received material, specimen annealed at 1050°C and 1200°C were 0.006430 %strain/s, 0.012821 %strain/s and 0.023643 %strain/s. The instantaneous strain of as-received, solution treated at 1050°C and solution treated at 1200°C were 0.008 %strain, 0.012 %strain and 0.064 %strain. The creep rate and

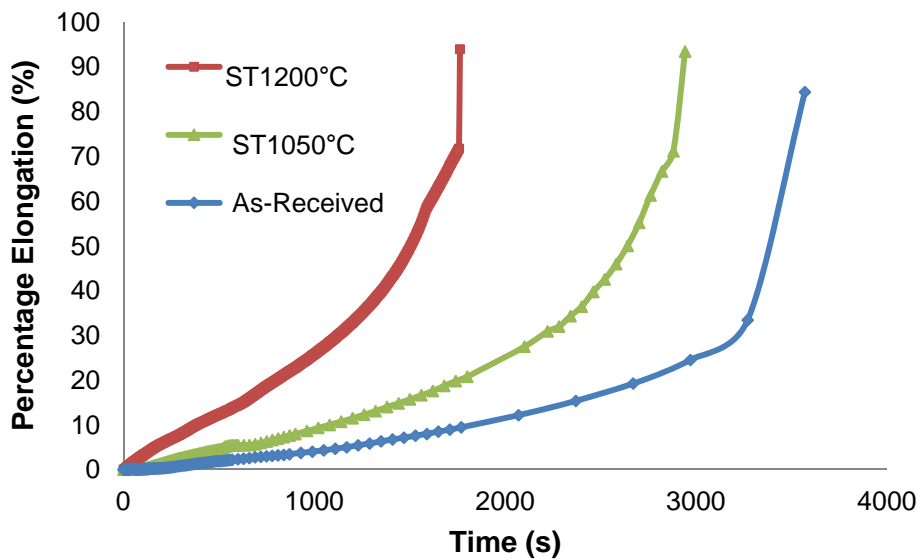instantaneous strain increase with increasing grain size.

Figure 3.4. The creep curve of alloy 800H at 900°C and 100MPa stress.

Figure 3.5 show the relationship between grain size and steady state creep rate. The steady state creep rate is directly proportional to the grain size. As grain size increase the creep resistance will decrease, this is because grain boundaries react as barrier to dislocation movement. The increase in steady state creep rate from 95.47µm to 380.95µm was dominated by the role of the barrier to the dislocation loop which was generated by cross slip (Lee 2001). The stress required to move a dislocation from one grain to another in order to plastically deform a material depends on the grain size. So, less force is needed to move a dislocation from a larger than from a smaller grain, leading materials with smaller grains to exhibit higher yield stress (Mittal 2009). A lower number of dislocations per grain results in a lower dislocation 'pressure' building up at grain boundaries. This makes it more difficult for dislocations to move into adjacent grains.
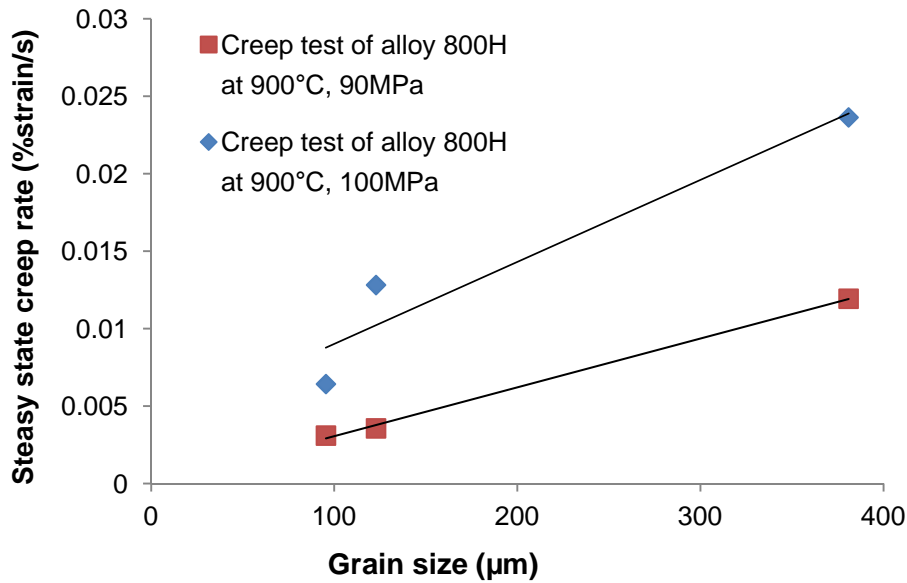
Figure 3.5. Plot of steady state creep rate vs. grain size at different stresses.

3.2 Fracture surface of creep test

Fracture surface of specimens underwent creep test at 900°C with stress of 90MPa are shown in Figure 3.6 and specimens undergone creep test at 900°C with stress of 100MPa are shown in Figure 3.7. All of the fracture surface exhibiting ductile fracture where cavities can be observed. These cavities eventually enlarge, propagate and link together forming a crack. The fracture surface shows ductile transgranular fracture mode and the surface appear rough and irregular which consists of many microvoids, crack and some dimples.

(a)   (b)   (c)
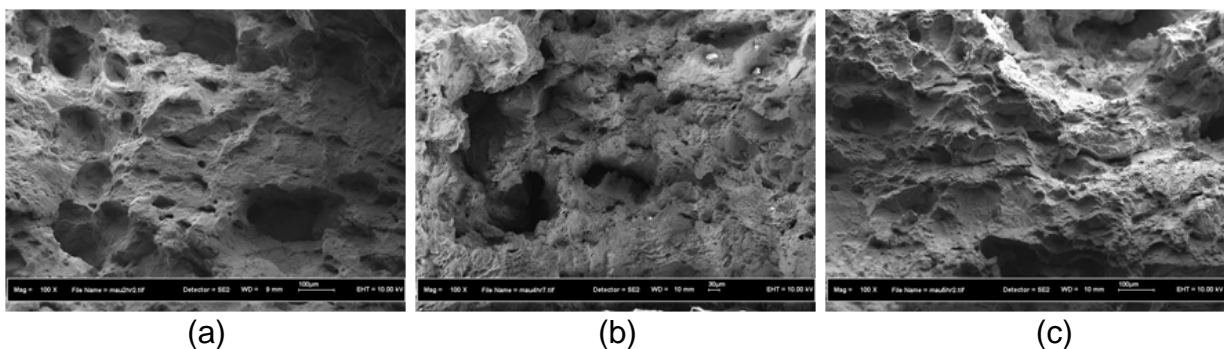
Figure 3.6. Fracture surface of specimen after creep test at temperature 900°C and 90MPa stress. (a) As-received; (b) Solution treated at 1050°C and (c) Solution treated at 1200°C.
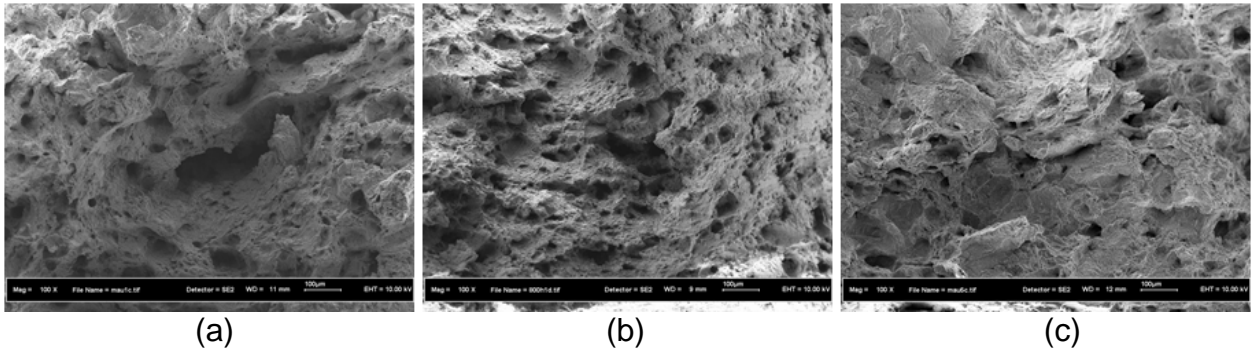
(a)	(b)	(c)

Figure 3.7. Fracture surface of specimen after creep test at temperature 900°C and 100MPa stress. (a) As-received; (b) Solution treated at 1050°C and (c) Solution treated at 1200°C.

3.3   Microstructure analysis of creep test

Figure 3.8 shows the location description for images taken from specimens after creep test at temperature 900°C and stresses at 90MPa and 100MPa.
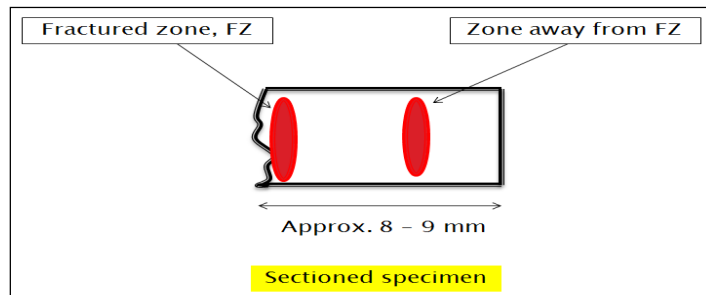

Figure 3.8. Zone description of image taken for fractured samples after creep test at temperature 900°C and stresses at 90MPa and 100MPa.

Figure 3.9 and Figure 3.10 show grain elongation which is parallel to the direction of the stress applied. It can be observed that the fracture transmit through the grain (transgranular fracture) for three of the different grain size of specimens. Precipitates TiN and TiC (Dehmolaei 2009, Dehmolaei 2008) still found in matrix and grain boundaries after creep test as can be seen in Figure 3.11. Mostly of the microvoids initiation occur at the grain boundaries show in Figure 3.12 and followed by linkage of microvoids to form a crack propagate across the grain finally cause failure to the specimens.
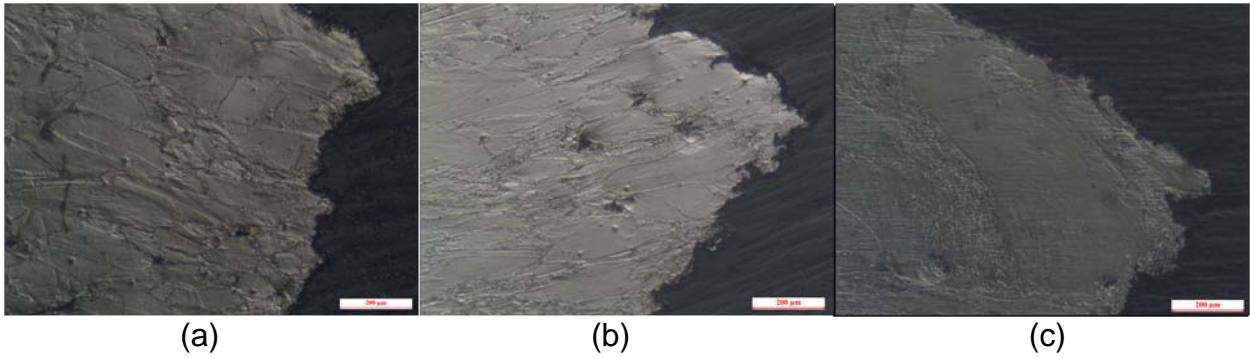
(a)   (b)   (c)

Figure 3.9. Cross section microstructure of the specimens after creep test at temperature of 900°C and 90MPa stress. (a) As-received; (b) Solution treated at 1050°C and (c) Solution treated at 1200°C.
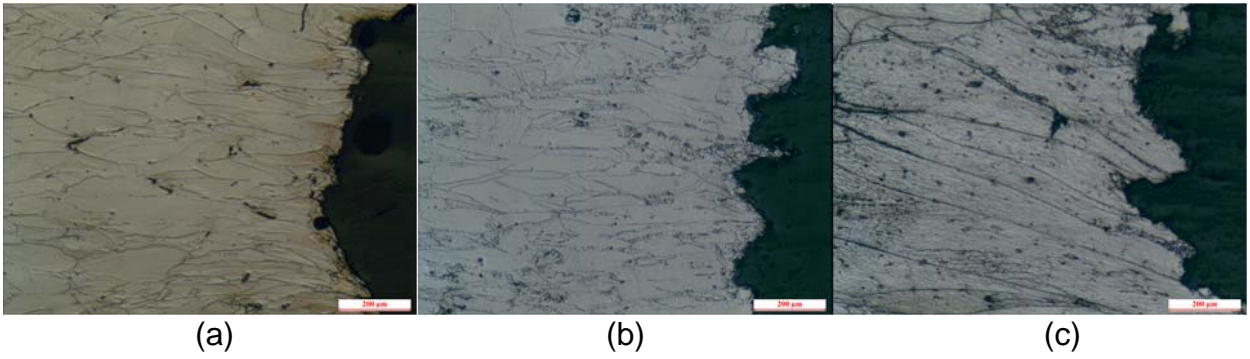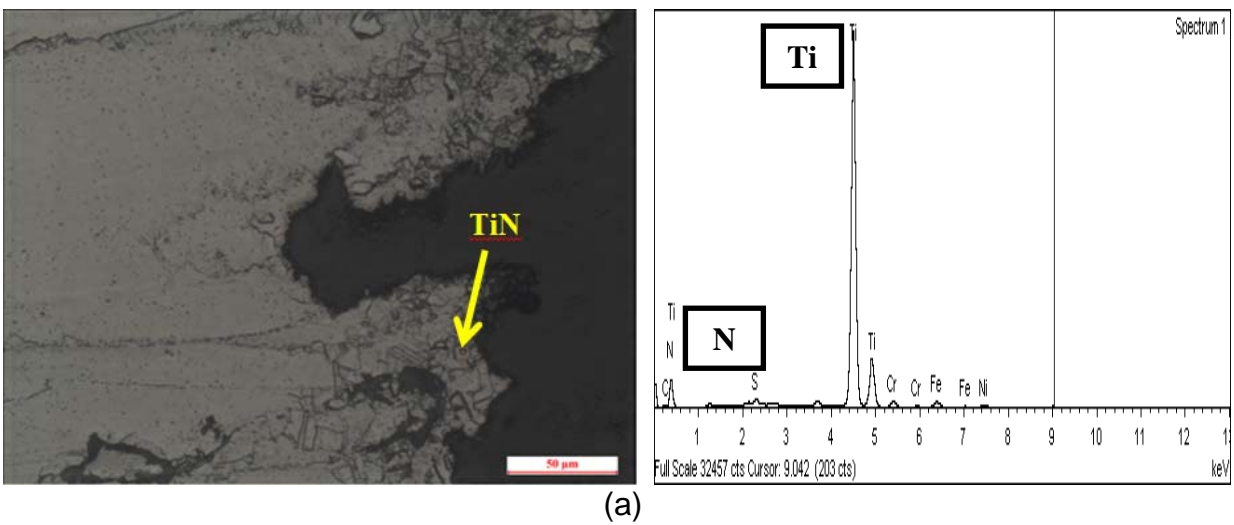

(a)   (b)   (c)

Figure 3.10. Cross section microstructure of the specimens after creep test at temperature of 900°C and 100MPa stress. (a) As-received; (b) Solution treated at 1050°C and (c) Solution treated at 1200°C.
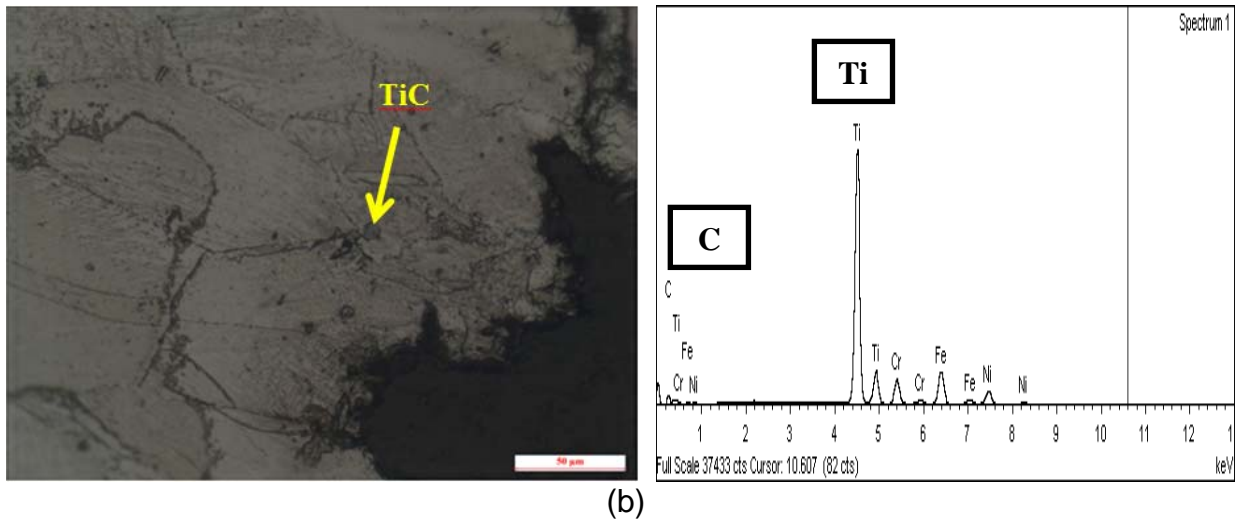

(a)

(b)

Figure 3.11. High magnification microstructure on fracture area after creep test. (a) 200X magnification on TiN precipitate and (b) 200X magnification on TiC precipitate.

Figure 3.12 shows the microstructures of the zone far from fracture area of as-received material, samples underwent solution treated at 1050°C and solution treated at 1200°C after creep tests. It show less grain elongation compare to fracture area. It was observed that some cavities form at the grain boundaries.

(a)   (b)   (c)
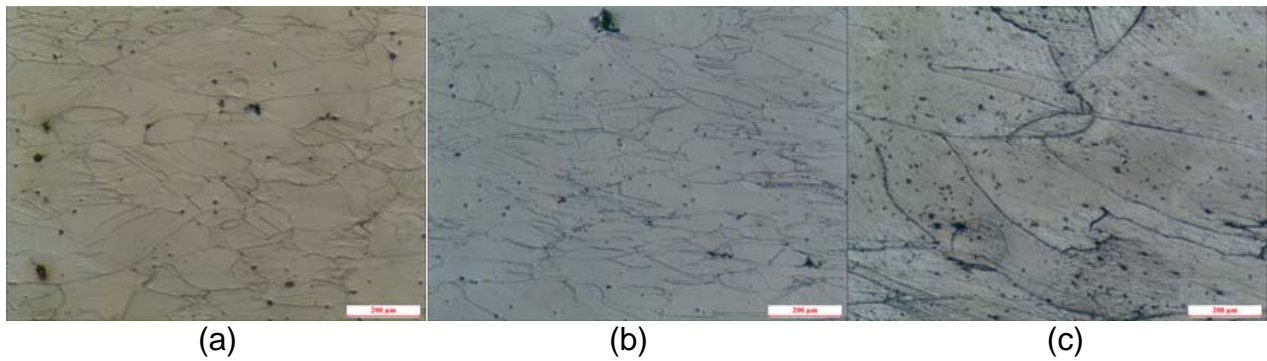
Figure 3.12. Microstructure at the zone far from fracture area after creep test at 100Mpa. (a) As-received; (b) Solution treated at 1050°C and (c) Solution treated at 1200°C.

4. CONCLUSIONS

The creep curve exhibiting primary, secondary, and tertiary stage creep. However, the curve becomes parabolic-like as grain size increases with constant load (90 MPa

and 100MPa) at temperature 900°C. The steady state creep rate increase with increase grain size due to the grain boundaries react as the barrier to the dislocation movement.

The alloy exhibit ductile transgrunular fracture during high temperature testing. The cavity and void formation took place at the grain boundaries followed by cavities linkage, crack formation and crack propagation through the grain until fracture.

REFERENCES

Chateau, E. and Remy, L. (2010), "Oxidation-Assisted Creep Damage in a Wrought Nickel-Based Supperalloy: Experiments and Modelling." Materials Sceience and Engineering A, Vol 527, 1655-1664.

Tresa, M.P. and Sammy, T. (2006), "Nickel-Based Superalloys for Advanced Turbine Engines: Chemistry, Microstructure, and Properties, Propulsion and Power." Vol 22, 361–374.

Hui, X.D., Yang, Y.S., Wang, Z.F., Yuan, G.Q. and Chen, X.C. (2000), "High temperature creep behavior of in-situ TiC particulate reinforced Fe–Cr–Ni matrix composite." Materials Science and Engineering A, Vol 282, 187–192.

Dehmolaei, R., Shamanian, M. and Kermanpur, A. (2009), "Microstructural Changes and Mechanical Properties of Incoloy 800 after 15 years service." Materials Characterization, Vol 60, 246-250.

Gan, J., Cole, J.I., Allen, T.R., Shutthanandan, S. and Thevuthasan, S. (2006), "Irradiated microstructure of alloy 800H." Journal of Nuclear Materials, Vol 351(1-3), 223-227.

Tan, L., Sridharan, K. and Allen, T.R. (2006), "The effect of grain boundary engineering on the oxidation behavior of Incoloy alloy 800H in supercritical water." Journal of Nuclear Materials, Vol 348(3) 263-271.

Abe, F., Kern, T. and Viswanathan, R. (2008), "Creep-resistant steels." England: Woodhead Publishing Limited.

Shingledecker, J.P. (2012), "Metallurgical Effects on Long-Term Creep-Rupture in a New Nickel-Based Alloy." The University of Tennessee, Knoxville.

Bernasconi, G. and Piatti, G. (1979), "Creep of Engineering Materials and Structures." London: Applied Science Publishers Ltd.

Lee, Y.S., Kim, D.W., Lee, D.Y. and Ryu, W.S. (2001), "Effect of Grain Size on Creep Properties of Type 316N Stainless Steel." Metals and Meterials International, Vol 7, 107-114.

Voicu, R., Lacaze, J., Andrieu, E., Poquillon, D. and Furtado, J. (2009), "Creep and Tensile Behaviour of Austenitic Fe–Cr–Ni Stainless Steels." Materials Science and Engineering A. Vol 510–511, 185 – 189.

Dehmolaei, R., Shamanian, M. and Kermanpur, A. (2008), "Microstructural Characterization of dissimilar welds between alloy 800 and HP heat-resistant steel." Materials Characterization, Vol 59, 1447-1454.

Mittal, R., (2009), "Strengthening Mechanism of Metals." Matellurgy and Materials Engineering, National Institute of Technology Rourkela.